

Finite Element Analysis and Experimental Study of the Ultrasonic Vibration-assisted Single Point Incremental Forming (UVaSPIF) Process

M. Vahdati*

Faculty of Mechanical and Mechatronics Engineering, Shahrood University of Technology, Shahrood, Iran

ARTICLE INFO

Article history:

Received 5 February 2019

Revised 4 July 2019

Accepted 24 August 2019

Keywords:

Incremental Forming
 Ultrasonic Vibration
 Finite Element Analysis
 Friction Force
 Forming Force

ABSTRACT

The mechanism of the Single Point Incremental Forming (SPIF) process is based on the localized plastic deformation of a sheet metal using a hemispherical-head tool that follows the path programmed into the controller of a CNC milling machine. In this process, no die is used under the sheet metal for support. The researchers' findings show that by applying ultrasonic vibration to forming processes, metallic samples are subject to plasticization, transiently and considerably. The beneficial results of applying ultrasonic vibration to the forming processes are due to the volume and surface effects that are related to a change in the properties of the material and also in frictional conditions. In this article, the Ultrasonic Vibration-assisted Single Point Incremental Forming (UVaSPIF) process was simulated in finite element software. The results of the numerical analysis showed that the ultrasonic excitation of the forming tool and an increase in the vibration amplitude reduced the friction force and the vertical component of the forming force. In the following, the results of the simulation process were compared with the experimental results at a frequency of 20 kHz and 7.5 μm vibration amplitude. The study of the results showed good congruence between the values of the vertical component of the forming force resulting from the numerical analysis and the experimental test.

© Shiraz University, Shiraz, Iran, 2019

1. Introduction

Researchers have shown that the application of high-frequency ultrasonic energy during tension and compression tests of metals reduces the material's yield strength [1-4]. The findings of Blaha and Langenecker [5] show that the changes in the mechanical properties during the tension accompanied with the ultrasonic excitation are due to the activation of dislocations. This can be ascribed to the fact that ultrasonic vibration is preferably absorbed in dislocations whose activation reduces the forming forces.

Huang et al. [6] conducted experimental studies on the ultrasonic-assisted upsetting. They found that ultrasonic vibration reduced the average forming force during the process due to the reduction of the friction

force. Li and Lang [7] reported the reduction of the forming force in an ultrasonic-assisted wire drawing. They realized that applying ultrasonic vibration improved the lubrication conditions between the wire and the mold. Ashida and Aoyama [8] conducted numerical and experimental studies on the pressing process using ultrasonic excitation of the mold. They found that using this energy could prevent the occurrence of wrinkling and cracks in the formed specimens. The results showed that this was due to the reduction of the friction force between the sheet metal and the mold.

Akbari Mousavi et al. [9] used the finite element method to investigate the effect of ultrasonic vibration on the average forming force in the forward extrusion. They showed that if the extrusion speed was less than the

* Corresponding author

E-mail address: vahdati@shahroodut.ac.ir (M. Vahdati)

critical speed, the extrusion force and the flow stress of the material under the influence of ultrasonic vibration were reduced. Djavanroodi et al. [10] examined the effect of ultrasonic vibration on the ECAP process using the finite element method and experiential test. They showed that by increasing the amplitude of the vibration and the ultrasonic frequency, the forming force reduced considerably. Ahmadi and Farzin [11] studied the effect of ultrasonic vibration on the ECAP process using a rigid and an elastic punch in finite element software. They showed that the reduction of the forming force depended on the vibration amplitude and the mold speed. Faraji et al. [12] studied the effect of ultrasonic vibration on the TCAP process using the finite element method. They showed that applying ultrasonic vibration to the radial direction of the mandrel was more effective than to the axial direction. This can lead to a reduction in the forming force and an increase in the plastic strain.

Vahdati et al. [13] developed the Ultrasonic Vibration-assisted Single Point Incremental Forming (UVaSPIF) by applying ultrasonic vibration to the hemispherical-head tool. They found that the application of ultrasonic vibration resulted in a reduction of the vertical component of the forming force, reducing the spring-back and improving the surface quality of the sample. Pengyang et al. [14] examined, both numerically and experimentally, the effect of ultrasonic vibration amplitude during the SPIF of a truncated cone. They reported that as the vibration amplitude increased, the forming force and the surface roughness of the sample decreased. Toshiyuki and Mamoru [15] developed the ultrasonic-assisted incremental microforming. They showed that the simultaneous application of ultrasonic vibration and laser heating improved the forming limit and shape accuracy of the formed specimen. Sakhtemanian et al. [16] suggested a new theoretical model based on the conversion of ultrasonic vibration to heat. According to this model, the tool's temperature increased quickly in the initial stages of the vibration and then reached a constant value. The presented model was used as the definition of material behavior (bimetal sheet) in the FE software. Furthermore, the experimental results showed the reduction of the amount of the force and coefficient of the friction under the effect of ultrasonic vibration.

It should be noted that the reduction of the forming

force leads to the reduction of the applied pressure on the spindle of NC or CNC milling machine. This matter is important in relation to the forming of high strength sheet metals and lightweight alloys (such as AA2024, AZ31B, and Ti6Al4V) at room temperature. On the other hand, no attempts have been made to conduct the finite element analysis on the effect of ultrasonic vibration on SPIF. Therefore, in this study, the research has focused on applying ultrasonic vibration to SPIF for numerically investigating the resulting deformation mechanism. Hence to simulate the experimental test and review the presented results in reference 13, the numerical modeling and analysis of the UVaSPIF process were performed for the first time on the Al 1050-O sheet. The results of the finite element analysis showed that the ultrasonic excitation of the forming tool and increasing the vibration amplitude reduced the friction force and the vertical component of the forming force in the straight groove test. Therefore, the surface effect of ultrasonic vibration was introduced as an effective mechanism to reduce the vertical component of the forming force. In addition, under the same conditions ($f = 20 \text{ kHz}$, $a = 7.5 \mu\text{m}$), the numerical and experimental values of the vertical component of the forming force were very well matched.

2. Description of the Finite Element Model

The finite element method is one of the numerical methods used to analyze the physical problems. Due to the widespread use of computer in engineering sciences, the finite element software has been developed based on the finite element method. In this study, ABAQUS 6.14 [17] was used to model and analyze the forming process. Since the wave of ultrasonic vibration was generated at a high speed, the finite element modeling was performed using explicit analysis procedure.

2.1. Modeling and meshing

The parts are modeled in a 3D manner based on the geometry and dimensions of the SPIF process components. The finite element model consists of a 10 mm hemispherical-head tool, a clamping plate, a sheet metal of $100 \times 100 \times 0.7$ mm in size, and a backing plate (Fig. 1).

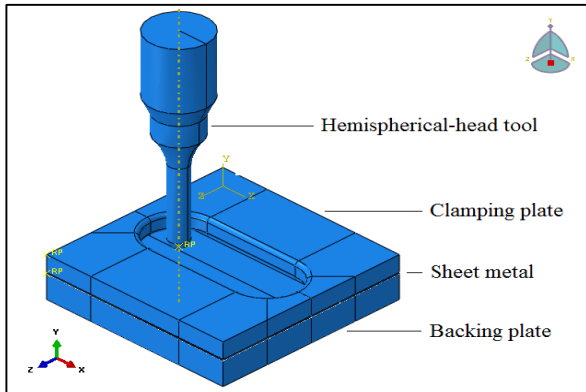
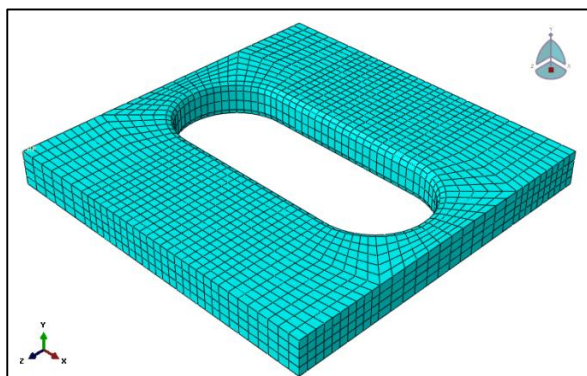
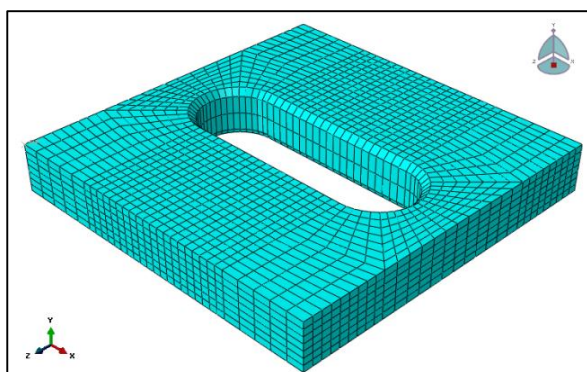


Fig. 1. Modeling the SPIF components

Given that, the material of the forming tool (stainless steel) is harder than that of the sheet metal (Al 1050-O); the tool was considered as an analytically rigid surface. Additionally, the clamping and backing plates were modeled as discrete rigid surfaces. The clamping and backing plates were modeled using the R3D4¹ element (Fig. 2).



(a) Clamping plate



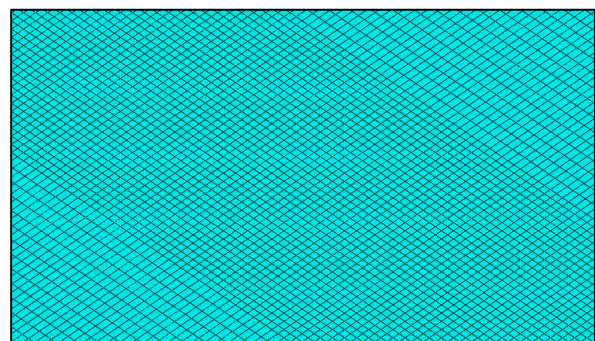
(b) Backing plate

Fig. 2. Meshing the rigid components of the SPIF fixture

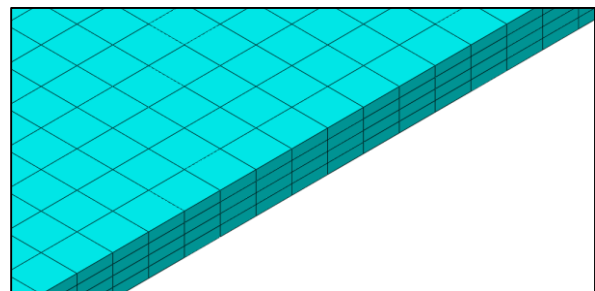
¹ Four-node bilinear rigid quadrilateral element

² Eight-node linear brick, reduced integration, and hourglass control element

On the other hand, the sheet metal was deformable and modeled using the C3D8R² element. A total of 69120 elements were generated using this model. The proper size of the element was selected based on the convergence of the maximum Von-Mises stress. Therefore, the middle area of the sheet (straight groove path) with an element size of 0.625 mm, the thickness of the sheet with an element size of 0.175 mm and other areas of the sheet with an element size of 2.5 mm were meshed (Fig. 3).



(a) Middle area



(b) Thickness area

Fig. 3. Sheet metal meshing

2.2. Material behavior

The plastic deformation behavior of the sheet metal follows the Hollomon's equation ($\sigma = K\varepsilon^n$). Hollomon's equation is a power law relationship between the stress and the amount of the plastic strain, where σ is the stress, K is the strength coefficient, ε is the plastic strain and n is the strain hardening exponent.

To determine the values of K and n , a tensile test was performed according to ASTM³ E8M-04 standard on Al 1050-O sheets at room temperature. For this purpose, standard specimens were prepared by the wire-EDM

³ American Society for Testing and Materials

machine in three directions of 0°, 45° and 90°. Then, each of the specimens was tested using an INSTRON tensile machine with a feed rate of 2 mm/min. The relationship between the true stress and true strain was extracted as $\sigma (MPa) = 140\varepsilon^{0.27}$. Table 1 shows the physical and mechanical properties of Al 1050-O sheet.

Table 1. Physical and mechanical properties of Al 1050-O sheet

Property	Symbol	Value
Density	ρ	2705 kg/m ³
Elastic modulus	E	69 GPa
Poisson's ratio	ν	0.33
Yield strength	$\sigma_{y0.2}$	28 MPa
Strength coefficient	K	140 MPa
Strain hardening exponent	n	0.27

2.3. Contact definition

To determine the frictional behavior of common surfaces, the Coulomb model was considered with a constant friction coefficient². The tool-sheet interface was defined as surface-to-surface contact.

To determine the best approximation for the coefficient of friction of the tool-sheet interface in a non-lubricating condition (dry friction), the simulation of the SPIF process for three different coefficients of friction of 0.15, 0.25 and 0.35 was performed under similar conditions. Based on the comparison of the forming forces resulted from the simulation and experimental tests, the coefficient of friction of 0.25 was selected as the best approximation. Therefore, the finite element model during the simulation processes uses this value to define the coefficient of friction at the tool-sheet interface.

2.4. Boundary conditions

The degrees of freedom of the clamping and backing plates along with the side faces of the sheet metal were fixed using the ENCASTRE boundary condition. The rotational speed of the forming tool was considered equal to 13 rad/s (125 rpm). The path travelled by the forming tool included 10 equal penetrations with a vertical step size of 0.5 mm and 10 linear paths with a

length of 50 mm. The final geometry is in the form of a straight groove (Fig. 4).

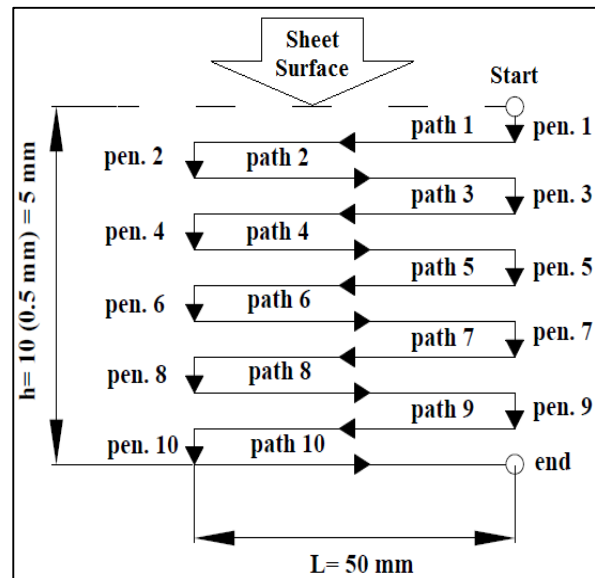


Fig. 4. Tool path strategy

The simulation of the UVaSPIF was performed by applying longitudinal vibration to the axis of the forming tool (Fig. 5). An ultrasonic oscillation with a frequency of 125664 rad/s (20 kHz) and amplitude of 7.5 μm is defined using a periodic function as a sine displacement ($u = a \sin \omega t$) (Fig. 6).

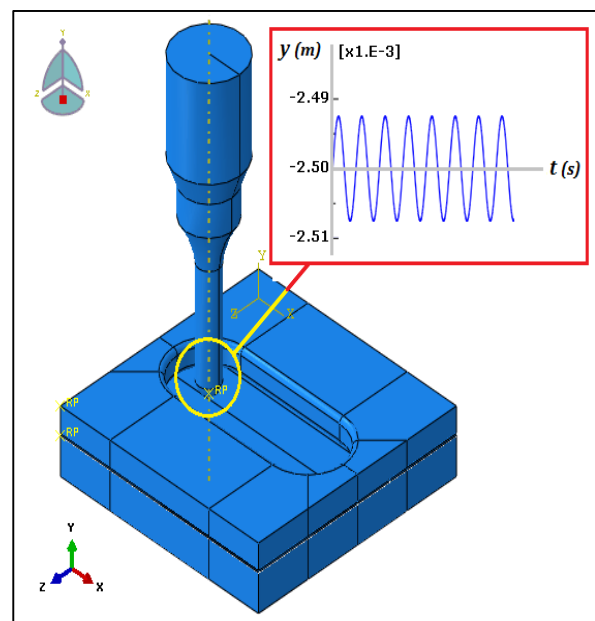


Fig. 5. Application of ultrasonic vibration to the forming tool

¹ Penalty method

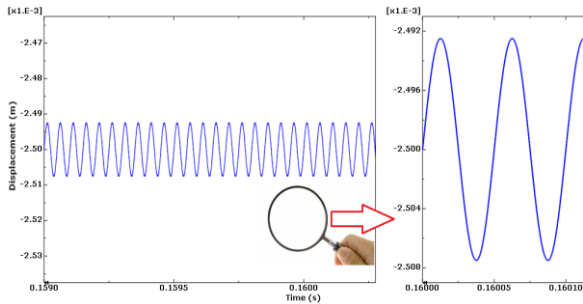


Fig. 6. Periodic oscillation of the forming tool ($a = 7.5 \mu\text{m}$)

2.5. Confirmation of the SPIF simulation

To confirm the simulation of the SPIF, the experimental forming was performed under similar conditions with the finite element analysis. The experimental setup for the SPIF is detailed in reference 13. Table 2 lists the input and common parameters of the simulation process and the experimental test.

Table 2. Input parameters of the simulation process and the experimental test

Parameter	Value
Sheet thickness	0.7 mm
Vertical step size	0.5 mm
Tool diameter	10 mm
Spindle speed	125 rpm

Figure 7 shows the comparison of the vertical component of the forming force (F_z) obtained from the simulation process and the experimental test for 10-fold stage tool paths. The vertical component of the forming force in the SPIF increases with the progression of the tool so that the plastic strain is applied to the specimen, and the sheet metal is deformed.

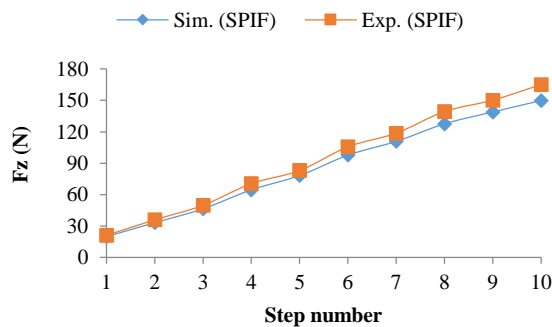


Fig. 7. Behavior of F_z in the simulation and experimental test of the SPIF

As can be seen, there is a slight difference (less than 8%) between the simulation and the experimental results. Consequently, the function of the finite element software is confirmed to simulate the SPIF and UVaSPIF processes.

2.6. Simulation of the UVaSPIF process

Regarding the confirmation of the simulation of the SPIF, the UVaSPIF simulation was performed by applying longitudinal vibration to the tool axis. The angular frequency and vibration amplitude are 125664 rad/s and $7.5 \mu\text{m}$, respectively (Fig. 8).

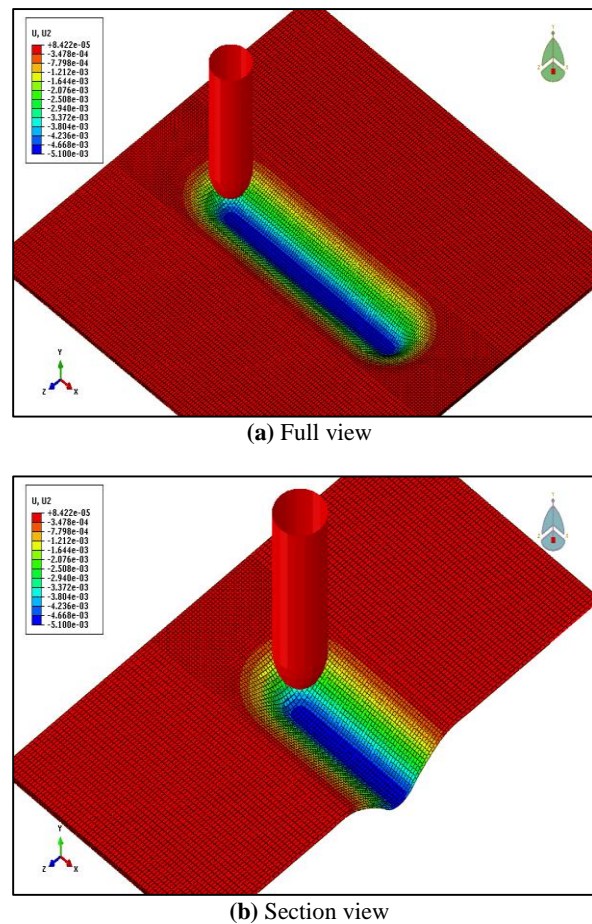


Fig 8. Formed sample in the UVaSPIF

As Figure 9 shows, the force behavior in the UVaSPIF is oscillating. Therefore, the force-time diagrams were calculated and extracted using a smooth function in the Abaqus software. This function uses the moving average algorithm to calculate the new values of the force.

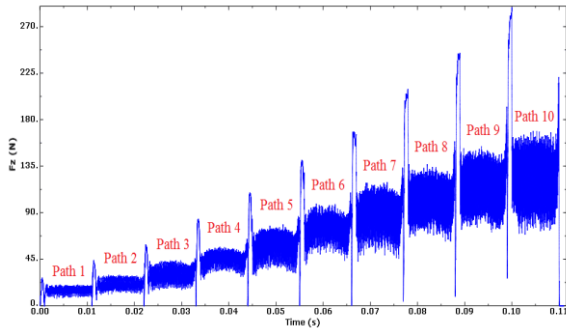


Fig. 9. Oscillatory behavior of the forming force in the UVaSPIF

3. Results of Numerical Analysis

3.1. Effect of ultrasonic vibration on the friction force

To extract the friction force in the SPIF and UVaSPIF, each of them must be simulated in two non-friction ($\mu = 0$) and friction ($\mu = 0.25$) conditions. The difference between the values of the horizontal component of the forming force (F_x) in two non-friction and friction conditions is considered as the friction force. (Fig. 10) shows the behavior of the F_x relative to the time in the SPIF and UVaSPIF in both "non-friction" and "friction" conditions during the fifth movement of the tool path (depth = 2.5 mm).

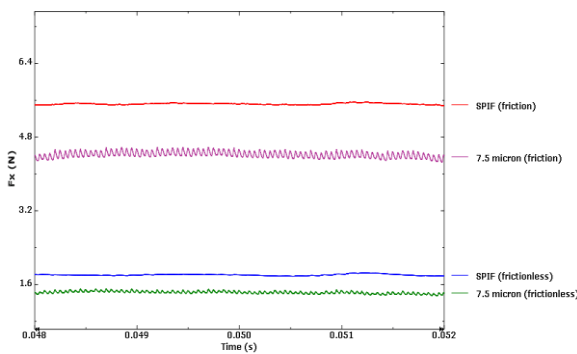


Fig. 10. $(F_x - t)$ diagram in the SPIF and UVaSPIF under friction and non-friction conditions

According to (Fig. 10), it is determined that the effect of applying ultrasonic vibration on the reduction of the F_x in the "friction" state is greater than that of the "non-friction" condition. By increasing the friction coefficient, the contribution of the friction force increases in the forming force. (Fig. 11) displays the difference between the $(F_x - t)$ curves of (Fig. 10). In other words, (Fig. 11) shows the friction force behavior (F_f) relative to the time for SPIF and UVaSPIF under common conditions.

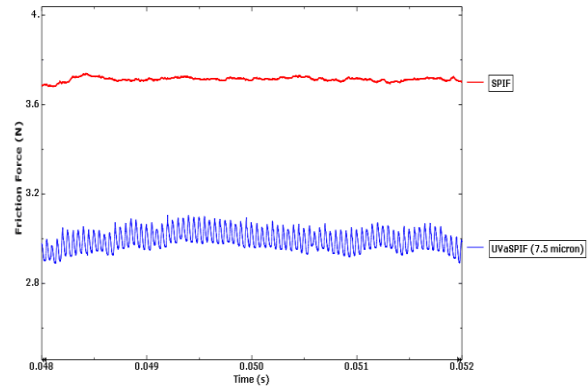


Fig. 11. $(F_f - t)$ diagram in the SPIF and UVaSPIF ($a = 7.5 \mu\text{m}$)

As can be seen, the friction force has been reduced by the effect of ultrasonic vibration compared to the SPIF. To investigate the friction force behavior on the 10-fold paths, the ratio of the friction force in the UVaSPIF ($F_{f_{ul}}$) to the friction force in the SPIF (F_f) was extracted (Fig. 12).

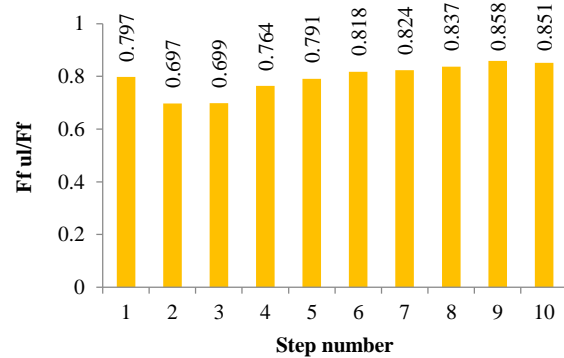


Fig. 12. Behavior of the ratio $\left(\frac{F_{f_{ul}}}{F_f}\right)$

As can be seen, the friction force in the UVaSPIF ($F_{f_{ul}}$) is, on the average, 79.4% of the friction force in the SPIF (F_f). In other words, the application of ultrasonic vibration to the forming tool reduces the friction force by approximately 20.6%.

3.2. Effect of the vibration amplitude on the friction force

To study the effect of the vibration amplitude on the friction force over the 10-fold paths, in addition to the $7.5 \mu\text{m}$ amplitude, the vibrational amplitudes of 2.5, 5 and 10 microns were applied at a constant frequency of 20 kHz. Then, the ratio of the friction force in different amplitudes of ultrasonic vibration ($F_{f_{ul}}$) to the friction force in the SPIF (F_f) was extracted (Fig. 13).

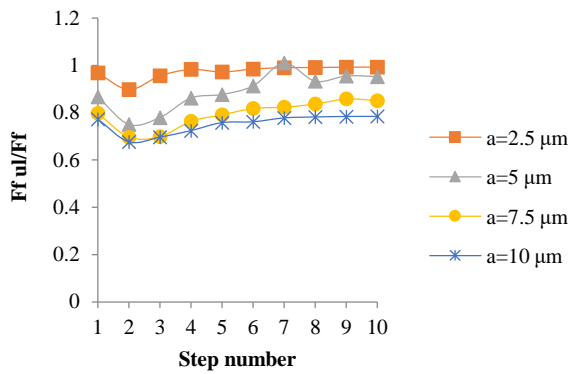


Fig. 13. Behavior of the ratio $\left(\frac{F_{zul}}{F_f}\right)$ for different amplitudes of ultrasonic vibration

As can be seen, increasing the vibration amplitude in the UVaSPIF will result in a further reduction of the friction force.

3.3. Effect of ultrasonic vibration on the vertical component of the forming force

Figure 14 shows the behavior of the vertical component of the forming force relative to the time in the SPIF and UVaSPIF during the fifth movement of the tool path (depth = 2.5 mm).

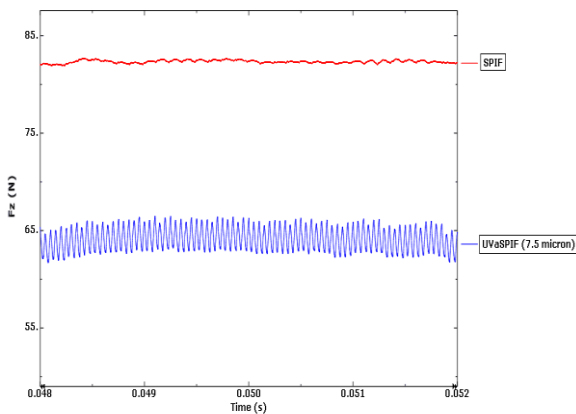


Fig 14. $(F_z - t)$ diagram in the SPIF and UVaSPIF ($a = 7.5 \mu m$)

As can be seen, the vertical component of the forming force has been reduced by the effect of ultrasonic vibration compared to the SPIF. To investigate the vertical component of the forming force behavior on the 10-fold paths, the ratio of the vertical component of the forming force in the UVaSPIF (F_{zul}) to the vertical component of the forming force in the SPIF (F_z) was extracted (Figure 15).

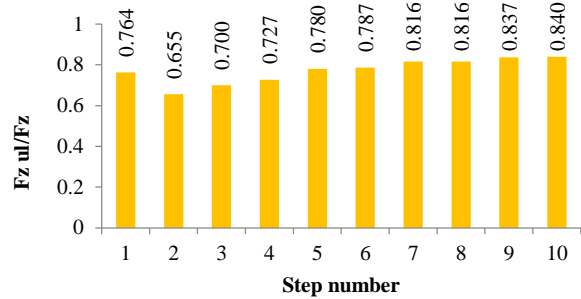


Fig. 15. Behavior of the ratio $\left(\frac{F_{zul}}{F_z}\right)$

As can be seen, the vertical component of the forming force in the UVaSPIF (F_{zul}) is, on the average, 77.2% of the vertical component of the forming force in the SPIF (F_z). In other words, the application of ultrasonic vibration to the forming tool reduces the vertical component of the forming force by approximately 22.8%.

3.4. Effect of the vibration amplitude on the vertical component of the forming force

To study the effect of the vibration amplitude on the vertical component of the forming force over the 10-fold paths, in addition to the 7.5 μm amplitude, the vibrational amplitudes of 2.5, 5 and 10 microns were applied at a constant frequency of 20 kHz.

Figure 16 shows the behavior of the vertical component of the forming force relative to the time for different amplitudes of ultrasonic vibration in the fifth movement of the tool path (depth = 2.5 mm).

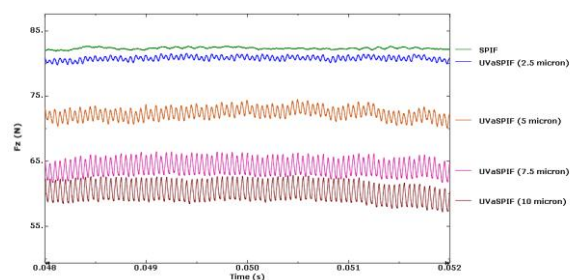


Fig. 16. $(F_z - t)$ diagram for different ultrasonic vibration amplitudes

As can be seen, increasing the vibration amplitude in the UVaSPIF will result in a further reduction of the vertical component of the forming force. To study the behavior of the vertical component of the forming force in the 10-fold paths, the ratio of the vertical component

of the forming force in different amplitudes of ultrasonic vibration (F_{zul}) to the vertical component of the forming force in the SPIF (F_z) was extracted (Fig. 17).

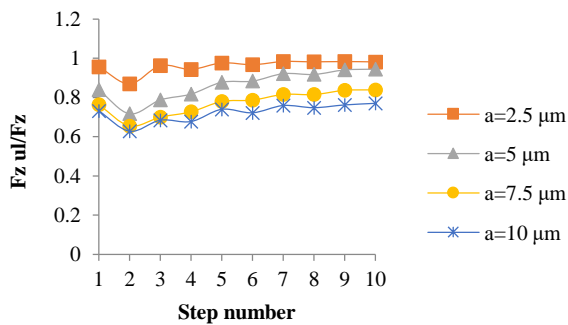


Fig. 17. Behavior of the ratio (F_{zul}/F_z) for different amplitudes of ultrasonic vibration

According to (Fig. 13 and 17), Table 3 presents the comparison of the reduction percentage of the friction force and the vertical component of the forming force in the UVaSPIF for different vibration amplitudes.

Table 3. Comparison of reduction percentage of F_{ful} and F_{zul} in the UVaSPIF for the different vibration amplitudes

Vibration amplitude (μm)	Reduction percentage of F_{ful} (%)	Reduction percentage of F_{zul} (%)
2.5	2.7	3.9
5	11	13.4
7.5	20.6	22.8
10	24.9	27.8

Therefore, it can be concluded that the vertical component of the forming force is reduced by the effect of reducing the friction between the vibrating tool and the sheet metal. In other words, changing the friction conditions between the vibrating tool and the sheet metal (surface effect of ultrasonic vibration) results in a reduction of the vertical component of the forming force.

4. Experimental Test

To apply ultrasonic vibration to the forming tool, a King generator with a power output of 1000 W at an operational frequency of 20 kHz was used. The ultrasonic generator converts low-frequency input voltage (220 VAC, 50–60 Hz) into high-frequency ultrasonic power (1000 W, 20 kHz). Experiments were

performed using a CNC horizontal milling machine at the University of Kashan (Fig. 18).

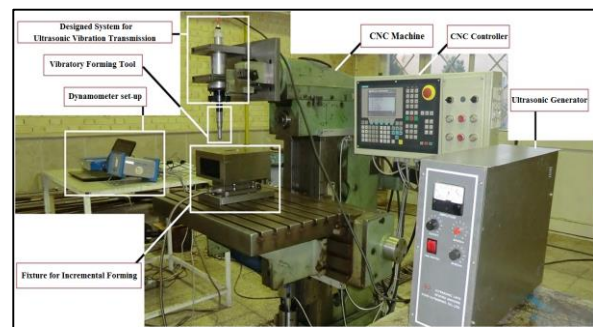


Fig. 18. Arrangement of the UVaSPIF components

In this study, ultrasonic energy was applied longitudinally to the forming tool so that it would vibrate. The principles of the design, analysis, fabrication, testing, and employment of the vibrating tool in the UVaSPIF are described in reference 13.

4.1. Experimental results

A Kistler piezoelectric dynamometer was employed to record the vertical component of the applied force (F_z) with the help of the Dynoware interface software. (Fig. 19) shows the mean values of the vertical component of the forming force in the SPIF (without vibration) and UVaSPIF (with vibration) over the 10-fold paths.

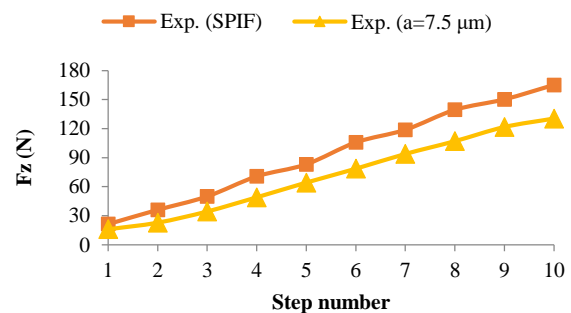


Fig. 19. Comparison between the mean values of F_z in the SPIF and UVaSPIF ($a = 7.5 \mu m$)

As can be seen, the ultrasonic excitation of the forming tool has reduced the mean values of the force applied to the tool axis. To study the procedure of the changes in the vertical component of the forming force in the 10-fold paths, the ratio of the vertical component of the forming force in the UVaSPIF (F_{zul}) to the vertical component of the forming force in the SPIF (F_z) was extracted (Fig. 20).

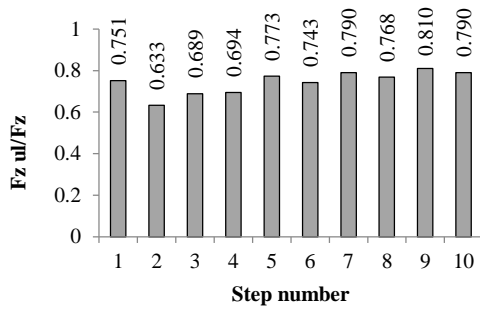


Fig. 20. Behavior of the ratio $\left(\frac{F_{zul}}{F_z}\right)$

As can be seen, the vertical component of the forming force in the UVaSPIF (F_{zul}) is, on the average, 74.4% of the vertical component of the forming force in the SPIF (F_z). In other words, the application of ultrasonic vibration to the forming tool reduces the vertical component of the forming force by approximately 25.6%.

4.2. Comparison and examination of the numerical and experimental values of the vertical component of the forming force

In this section, the common results obtained from the numerical analysis and experimental test are compared in two situations: "without vibration" and "with vibration". (Fig. 21) shows the comparison of the values of the vertical component of the forming force generated by the numerical analysis and by the experimental test [13] in the UVaSPIF ($f = 20 \text{ kHz}$, $a = 7.5 \mu\text{m}$).

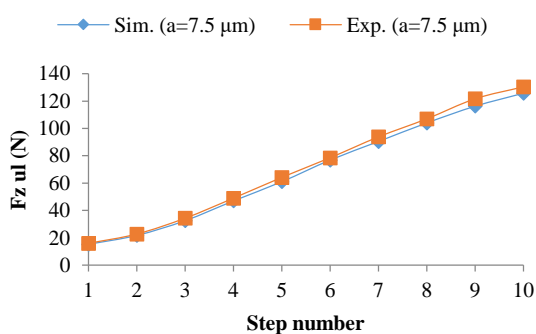


Fig. 21. Comparison of F_{zul} over the 10-fold paths of the UVaSPIF ($a = 7.5 \mu\text{m}$)

As can be seen, the difference between the numerical and experimental results of the UVaSPIF is less than 5%, suggesting a proper match between the numerical and experimental results. The factors that can be raised as the uncertain sources include:

- Using the approximate amount of dry friction coefficient in the FEA
- Discarding the effect of the localized increase of the temperature due to ultrasonic vibration at the tool-sheet interface
- Measuring the error of the vertical component of the forming force due to:
 1. Non-perpendicularity of the experimental set-up on the dynamometer surface
 2. The effect of the friction between the force transmission components
- Reduction of the ultrasonic vibration amplitude due to the tool-sheet contact

Table 4 shows the average of the reduction percentage of the vertical component of the forming force for each of the numerical and experimental analysis.

Table 4. Reduction percentage of the vertical component of the forming force

Analysis type	Reduction percentage (%)
Numerical	22.8
Experimental	25.6

As can be seen, the reduction in the vertical component of the forming force in the experimental test is more than that of the simulation process. This is due to the material softening during the experimental test, which, together with the surface effects of ultrasonic vibration, results in a further reduction of the forming force. Based on the numerical and experimental results, some of the effective factors in terms of force reduction in the UVaSPIF are as follows: frictional changes between the forming tool and the sheet metal, surface elastic-plastic deformation, dynamic effects of ultrasonic vibration and the changes in the material flow. Generally, all of these factors are associated with the surface effects of ultrasonic vibration [6, 8]. Consequently, the reduction in the vertical component of the forming force was mainly because of the surface effects, or changes in the tool-sheet contact conditions, and not because of the volume effects. It seems that, because of the ultrasonic effects, the surface elastic-plastic deformation increased the temperature at the tool-sheet interface. An increase in the temperature affects the material flow. Therefore, the vertical component of the forming force decreased.

5. Conclusion

In this research, the simulation of the UVaSPIF was performed in the finite element software. Then, the numerical analysis and experimental test results were compared and studied. The most important results of this research are listed below:

- The finite element analysis showed that the ultrasonic excitation of the forming tool ($f = 20 \text{ kHz}$, $a = 7.5 \mu\text{m}$) in the straight groove test reduced the friction force and the vertical component of the forming force by 20.6% and 22.8%, respectively.

- The effect of a reduction in the friction between the vibrating tool and the sheet metal resulted in a reduction of the vertical component of the forming force. In other words, changing the frictional conditions between the vibrating tool and the sheet metal (surface effect of ultrasonic vibration) reduces the vertical component of the forming force.

- Increasing the vibration amplitude in the UVaSPIF resulted in a further reduction in the friction force and the vertical component of the forming force.

- The experimental test showed that the application of ultrasonic vibration ($f = 20 \text{ kHz}$, $a = 7.5 \mu\text{m}$) reduced the vertical component of the forming force by approximately 25.6%.

- The reduction in the vertical component of the forming force in the experimental test (25.6%) is more than the simulation process (22.8%). This is due to the material softening during the experimental test, which, together with the surface effects of ultrasonic vibration, results in a further reduction of the forming force.

5. References

- [1] Langenecker, B. "Work-softening of metal crystals by alternating the rate of glide strain". *Acta Metallurgica*, 9 (1981) 937-940.
- [2] Langenecker B., "Effects of ultrasound on deformation characteristics of metals". *IEEE Transactions on Sonics and Ultrasonics*, 13 (1966) 1-8.
- [3] Bagherzadeh. S., Abrinia. K. "Effect of Ultrasonic Vibration on Compression Behavior and Microstructural Characteristics of Commercially Pure Aluminum". *Journal of Materials Engineering and Performance*. 24 (11) (2015) 4364-4376.
- [4] Haiyang, Z., Hongzhi, C., Qing, H.Q. "Influence of ultrasonic vibration on the plasticity of metals during compression process". *Journal of Materials Processing Technology*, 251 (2018) 146-159.
- [5] Blaha, F., Langenecker, B., "Tensile deformation of zinc crystal under ultrasonic vibration". *The Science of Nature*, 42 (20) (1955) 556.
- [6] Huang, Z., Lucas, M., Adams, M.J., 2002. "Influence of ultrasonics on upsetting of a model paste". *Ultrasonics*, 40 (2002) 43-48.
- [7] Li, L., Lang, X., "Wire drawing with ultrasonic vibration". *Journal Wire Industry*, 61 (1994) 721.
- [8] Ashida, Y., Aoyama, H., 2007. "Press forming using ultrasonic vibration". *Journal of Materials Processing Technology*, 187-188 (2007) 118-122.
- [9] Akbari Mousavi, S.A.A., Feizi, H., Madoliat, R., "Investigations on the effects of ultrasonic vibrations in the extrusion process". *Journal of Materials Processing Technology*, 187 (2007) 657-661.
- [10] Djavanroodi, F., Ahmadian, H., Koochkan, K., Naseri, R., "Ultrasonic-assisted ECAP". *Ultrasonics*, 53 (2013) 1089-1096.
- [11] Ahmadi, F., Farzin, M., 2013. "Finite element analysis of ultrasonic-assisted equal channel angular pressing". *Proceedings of the Institution of Mechanical Engineers, Part C: Journal of Mechanical Engineering Science*, 228 (11) (2013) 1859-1868.
- [12] Faraji, G., Ebrahimi, M., Bushroa, AR., "Ultrasonic assisted tubular channel angular pressing process". *Materials Science & Engineering: A*, 599 (2014) 10-15.
- [13] Vahdati, M., Mahdavinejad, R.A., Amini, S., "Investigation of the ultrasonic vibration effect in incremental sheet metal forming process". *Proceedings of the Institution of Mechanical Engineers, Part B: Journal of Engineering Manufacture*, 231 (6) (2015) 971-982.
- [14] Pengyang, L., Jin, H., Qiang, L., Mingshun, Y., Quandai, W., Qilong, Y., Yan, L., 2017. "Evaluation of forming forces in ultrasonic incremental sheet metal forming". *Aerospace Science and Technology*, 63 (2017) 132-139.

- [15] Toshiyuki, O., Mamoru, H., 2017. "Ultrasonic-Assisted Incremental Microforming of Thin Shell Pyramids of Metallic Foil". *Micromachines*, 8 (2017) 142, doi:10.3390/mi8050142.
- [16] Sakhtemanian, M.R., Honarpišeh, M., Amini, S. "A novel material modeling technique in the single-point incremental forming assisted by the ultrasonic vibration of low carbon steel/commercially pure titanium bimetal sheet". *International Journal of Advanced Manufacturing Technology*, 102 (1-4) (2019) 473-486.
- [17] Dassault Systèmes, www.3DS.com/simulia (2002, accessed 2019).

تحلیل المان محدود و مطالعه تجربی فرآیند شکل‌دهی تدریجی تک‌نقطه‌ای به کمک ارتعاشات اولتراسونیک (UVaSPIF)

مهدی وحدتی

دانشکده مهندسی مکانیک و مکاترونیک، دانشگاه صنعتی شاهرود، شاهرود، ایران.

چکیده

مکانیزم فرآیند شکل‌دهی تدریجی تک‌نقطه‌ای (SPIF) براساس تغییر شکل موضعی یک ورق فلزی با استفاده از یک ابزار سرنیمکروی می‌باشد که مسیر حرکت آن در کنترلر ماشین فرز CNC برنامه‌ریزی شده است. در این فرآیند، هیچ گونه قالبی به عنوان پشتیبان در زیر ورق استفاده نمی‌شود. یافته‌های محققان نشان می‌دهد که با اعمال ارتعاشات اولتراسونیک در فرآیندهای شکل‌دهی، نمونه‌های فلزی به صورت زودگذر و قابل توجهی در معرض نرم‌شدگی قرار می‌گیرند. نتایج سودمند اعمال ارتعاشات اولتراسونیک در فرآیندهای شکل‌دهی، ناشی از دو تأثیر حجمی و سطحی است که به ترتیب مرتبط با تغییر خواص ماده و تغییر شرایط اصطکاکی می‌باشد. در مقاله پیش‌رو، فرآیند شکل‌دهی تدریجی تک‌نقطه‌ای به کمک ارتعاشات اولتراسونیک (UVaSPIF) در نرم‌افزار المان محدود، شبیه‌سازی شد. نتایج حاصل از تحلیل عددی نشان داد که تحریک اولتراسونیک ابزار شکل‌دهی و افزایش دامنه ارتعاش موجب کاهش نیروی اصطکاک و کاهش مؤلفه عمودی نیروی شکل‌دهی می‌شود. در ادامه، نتایج حاصل از فرآیند شبیه‌سازی با نتایج حاصل از آزمون تجربی تحت فرکانس 20 kHz و دامنه ارتعاش 7.5 μm، مورد مقایسه و مطالعه قرار گرفت. بررسی نتایج نشان داد که مطابقت بسیار خوبی میان مقادیر مؤلفه عمودی نیروی شکل‌دهی حاصل از تحلیل عددی و آزمون تجربی برقرار می‌باشد.

واژه‌های کلیدی: شکل‌دهی تدریجی، ارتعاشات اولتراسونیک، تحلیل المان محدود، نیروی اصطکاک، نیروی شکل‌دهی.